Sideband-separating MMIC receivers for observation in the 3-mm band

James W. Lamb*[a], Kieran A. Cleary[a], Rohit S. Gawande[a,b], Jacob W. Kooi[a,b], Michael P. Laxen[a], Richard L. Plambeck[c], Rodrigo A. Reeves[d], Pekka P. Kangaslahti[b], Mikko Varonen[b,e]

[a]California Institute of Technology, 1200 E. California Blvd. Pasadena, CA, USA 91125; [b]Jet Propulsion Lab., 4800 Oak Grove Dr., Pasadena, CA 91109, USA; [c]University of California at Berkeley, Berkeley, CA 94720-3411, USA; [d]Univ. de Concepción, Victor Lamas 1290, Concepción, Chile; [e]Aalto Univ. School of Electrical Engineering, P.O. Box 11000, FI-00076, Aalto, Finland

ABSTRACT

Wideband receivers for the 3-mm band were developed for CARMA, the Combined Array for Research in Millimeter-wave Astronomy. Three cryogenic MMIC (monolithic microwave integrated circuit) amplifiers manufactured in InP 35-nm technology are combined in a block with waveguide probes and gain equalizers to cover the 80–116 GHz band. These are followed by a sideband-separating mixer that has two 17 GHz wide outputs, for upper and lower sidebands. Each receiver has a feed horn followed by a circular-to-linear polarizer and orthomode transducer. The two polarizations are amplified by the cryogenic MMICs, and the outputs downconverted in sideband separating mixers, resulting in four 1–18 GHz channels that can be simultaneously correlated. The first receiver was tested in the lab, and on-sky tests conducted at CARMA. Measured noise temperatures were in the range 40–70 K, with a sideband rejection of about 15 dB.

Keywords: Receivers, microwaves, millimeterwaves, sideband separation, interferometer, quadrature hybrid

1. INTRODUCTION

Historically, advances in millimeter instrumentation have emphasized low system temperatures, but this has reached a point of diminishing returns as the sensitivity becomes limited by the atmosphere for many ground-based observations. This, plus the ever increasing capabilities of digital correlators and spectrometers have made ultra-wideband instrumentation a very attractive avenue for technology advancement. CARMA[1] (Combined Array for Research in Millimeter-wave Astronomy) has operated for several years in the 75–116 GHz band with a combination of SIS (superconductor-insulator-superconductor) tunnel-junction mixers on the 10.4-m and 6.1-m antennas, and MMIC (monolithic microwave integrated circuit) amplifiers on the 3.5-m antennas. The instantaneous bandwidth is 8 GHz in a single polarization. In the case of the SIS mixers, which are double-sideband (DSB), the separation of the signal in the sidebands occurred in the correlator. Although the astronomical signal is cleanly separated, any noise from the atmosphere, ground spillover, or optical/waveguide losses is still combined from the two sidebands, with a corresponding noise penalty.

With these considerations in mind, it was decided to develop and field a receiver system that could produce two sidebands of 17 GHz in each of two polarizations. This total instantaneous bandwidth of 68 GHz per antenna is a factor of >8 relative to the existing technology. To achieve this, we needed to develop several components, including MMIC devices to cover this band, circular waveguide polarizers, and wideband sideband-separating mixers. In the following sections we present these developments, and discuss test results from the laboratory and on sky.

*lamb@caltech.edu; phone 1 760 853-6402; fax 1 760 938-2075; www.ovro.caltech.edu

Millimeter, Submillimeter, and Far-Infrared Detectors and Instrumentation for Astronomy VIII,
edited by Wayne S. Holland, Jonas Zmuidzinas, Proc. of SPIE Vol. 9914, 99140H
 · doi: 10.1117/12.2233106

1.1 Receiver architecture

Figure 1 presents the receiver architecture schematically. Signals passing through the dewar window in the 80–116 GHz band are captured by the corrugated feed horn and converted from circular to linear polarization. The two polarizations are separated in an orthomode transducer (OMT) before being amplified in MMIC amplifiers. After transmission out of the dewar in waveguide, the two polarizations are downconverted by sideband-separating mixers that provide the upper and lower sidebands in the IF (intermediate frequency) band at 1–18 GHz.

Because this was an upgrade project, we required that the new receivers should be compatible with the existing ones and the IF transmission system, making an incremental transition possible. Also, since the correlator was not slated to be expanded to accept the full bandwidth in the same proposal period, we included a tunable LO (local oscillator), to cover the whole RF range in steps. In any event, a tuning range of ±1 GHz would be required to fill in the central hole resulting from the 1-GHz minimum IF.

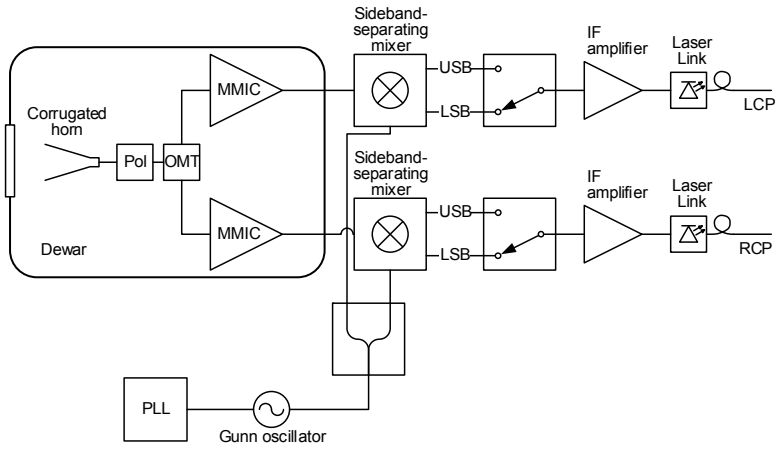

Figure 1. This shows the architecture of the new receiver. The first components are in the 4-K dewar, including the corrugated feed horn, circular-to-linear polarizer, orthomode transducer, and MMIC amplifiers. Stainless-steel waveguides carry the signal out of the dewar to the room-temperature sideband-separating mixers. In the initial implementation sidebands are selected by a co-axial switch before being amplified and sent to the correlator on a fiber link.

Figure 2 shows the downconversion scheme for the final and intermediate configurations. In the final scheme (Figure 2a) the entire band from 80–116 GHz can be processed, apart from a region of ±1 GHz about the LO which results from the 1 GHz minimum IF frequency. This can be covered with a slight shift in the LO. In Figure 2b, the intermediate configuration that is compatible with the existing 1–9 GHz IF range is shown with two tunings that cover most of the band. In fact, the current system has only two channels with an 8-GHz bandwidth, so each polarization can have only the upper sideband (USB), or lower sideband (LSB) selected at any one time. This implies a slight incompatibility with the existing system in which the two sidebands are transmitted in the same IF and separated in the correlator.

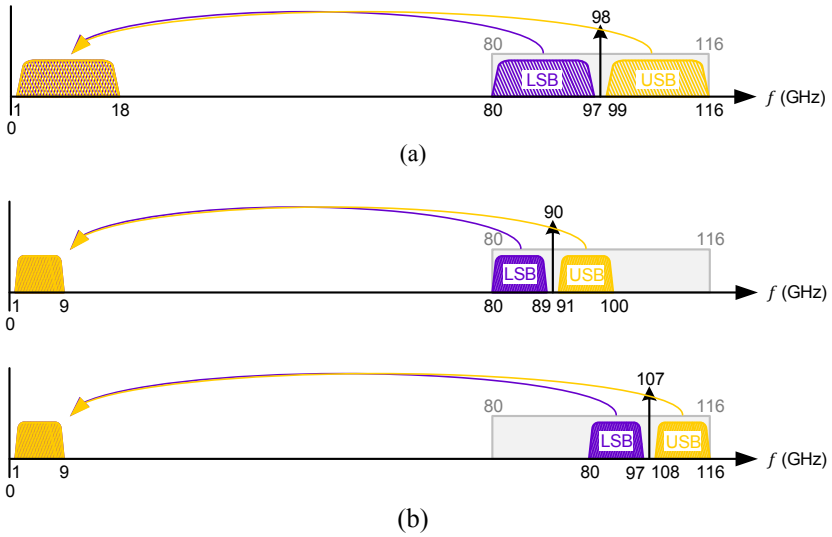

Figure 2. Schematic depiction of the frequency conversion schemes. (a) The whole band from 80–116 GHz, apart from a 2-GHz hole in the middle, is converted down to an IF frequency of 1–18 GHz. (b) With the existing IF system, only 8 GHz (1–9 GHz) can be handled, necessitating some tuning of the LO to cover the input band. In both these schemes, the USB and LSB are separated in the mixer.

2. DEWAR COMPONENTS

2.1 MMIC amplifiers

Prior developments[2] of amplifiers by JPL, CRAL, and Northrop Grumman Corporation (NGC) had yielded MMICs with close to the required performance for CARMA. Further refinement of these devices to remove a dip in response at the high end due to an air-bridge for a bias line, and improvement of the gain flatness with a better transistor noise model resulted in amplifiers that had excellent characteristics for this project.

The amplifiers were designed in NGC's 35-nm InP MMIC technology node, using InAs composite channel HEMTs that have demonstrated maximum oscillation frequencies above 1 THz. The process has scaled passive components and device passivation. The wafer is thinned down to 50 μm with a metal back-plane to suppress substrate modes. The amplifiers utilize two gate finger devices, and grounded coplanar waveguide transmission lines were used for on-chip matching. Each chip has three HEMTs with interstage matching.

Measurements of chip performance was expedited by the CRAL cryogenic probe station[3], allowing chips to be screened before incorporation into amplifier blocks. Measurements of *s*-parameters agreed well with room-temperature measurements, adjusted for the expected changes in device mutual conductance and capacitance. Although the noise measurements showed some systematic differences compared to mounted devices, the relative performance was sufficient for the selection process.

Achieving sufficient gain to make the contributions of later components was found to require three MMICs. This included allowances for gain equalizing connections between stages to flatten out some of the amplifier gain variations and to introduce some return-loss isolation, reducing ripple. Models of the block were built in HFSS (Ansys, Inc) with ports corresponding to the input and output ports on each of the MMIC chips and interstage networks. The input and output waveguide probes were part of the HFSS model. By combining the HFSS model *s*-parameters, the measured MMIC *s*-parameters, and models of the equalizers in Sonnet, the equalizers could be optimized for optimum gain flatness.

Critical issues that were identified were the lengths of the wire bonds, and the location of the chips, including MMICs, probes and equalizers.

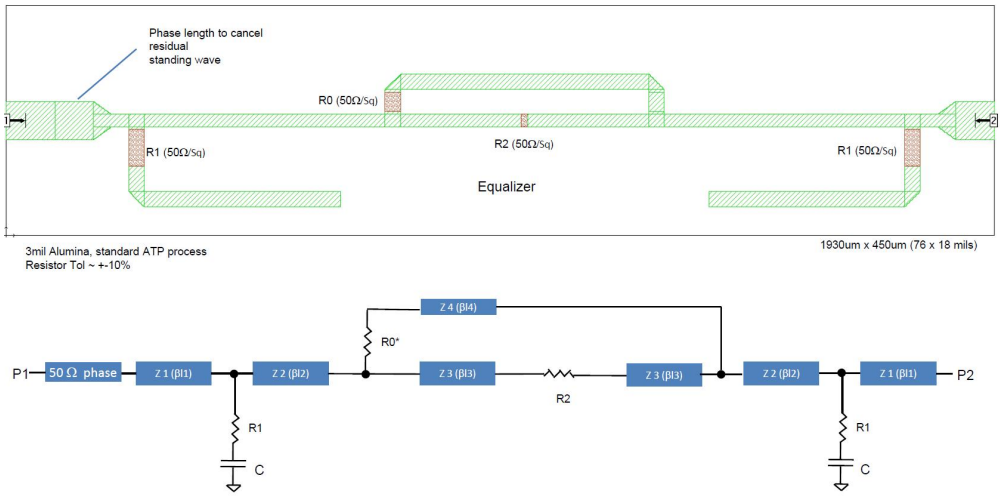

Figure 3. Typical layout and schematic for an interstage equalizer for the MMIC amplifiers. These were fabricated on 76 μm thick alumina substrate.

The amplifier blocks were machined from naval brass in a split-block configuration, with the split in the E-plane. Blocks were gold plated after lapping. Each MMIC was glued into its cavity with silver epoxy, and the connecting channels between chips and bias lines were made as narrow as possible to eliminate waveguide modes that could lead to instabilities due to feedback. Aggressive protection was designed into the bias circuit[4], including a 10:1 divider on the gate supplies to reduce the effects of noise and ground current offsets.

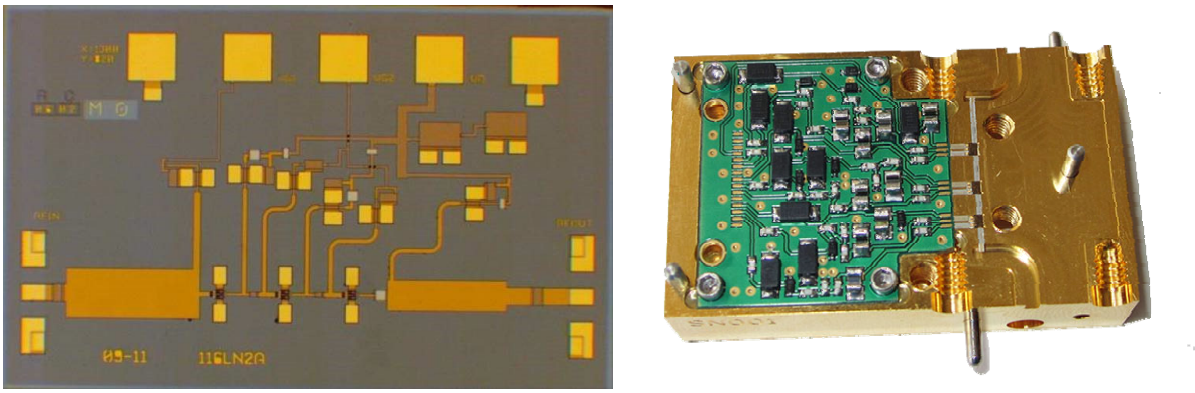

(a) (b)

Figure 4. (a) A photo of one of the MMIC chips, showing the bias bond pads (top), input pad (left), output pad (right) and the three HEMTs. (b) Photo of the lower half of an amplifier block with the bias protection circuit (left), and the three MMIC chips with input and output probes, and interstage matching elements.

Cryogenic testing was done with both a vector network analyzer, and a specially developed waveguide load with a temperature-variable metallized quartz vane.

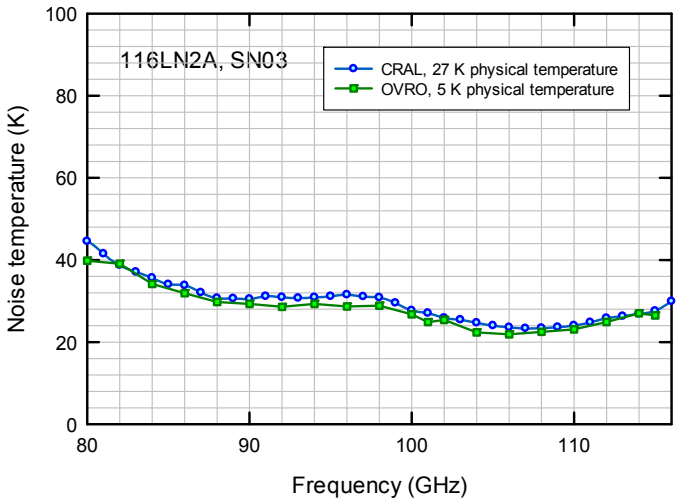

Figure 5. Noise measurements made on an amplifier block at the Cahill Radio Astronomy Lab (CRAL) and the Owens Valley Radio Astronomy (OVRO). The agreement between the two measurements made by different people with different test setups gives good confidence in their accuracy. Note that a small improvement in noise is afforded by the lower temperature in the OVRO 4-K cryostat.

2.2 Waveguide polarizer

Based on the same principles as the CARMA 1-mm polarizer[5], the 3-mm polarizer is built in circular guide with flat facets cut into the walls at three positions along the guide. The lengths of these facets and their rotation around the waveguide axis were optimized to give good circularity across the whole waveguide band.

2.3 Orthomode transducer

Orthomode transducers designed by Henke and Claude[6] were purchased from the Hertzberg Institute for Astronomy. Designed for application in ALMA, these have nearly ideal performance for the CARMA receivers.

2.4 Waveguide thermal break and vacuum window

These components were purchased from Aerowave. 25 μm thick Mylar was used as the window material. The stainless guide was unplated internally, and the loss of 1.5–2.0 dB across the band for the guide and window adds only a small amount to the system temperature since they follow the amplifiers.

3. SIDEBAND-SEPARATING MIXER

In communications and other microwave applications image-reject mixers (IRM) are commonly used to obtain single-sideband (SSB) response. Astronomical applications often require both sidebands to be utilized to get the greatest throughput; these are referred to as sideband-separating, or two-sideband (2SB) mixers. The method is identical to that of IRMs, except that both sidebands are retained. There are a couple of reasons for choosing this configuration over a single-sideband system. One is that, for a given RF bandwidth, the IF bandwidth is halved, which can make some of the components more practicable. The other is that tuning is achieved simply by changing the LO frequency, rather than having to have a tunable filter that can be difficult to implement in the millimeter region.

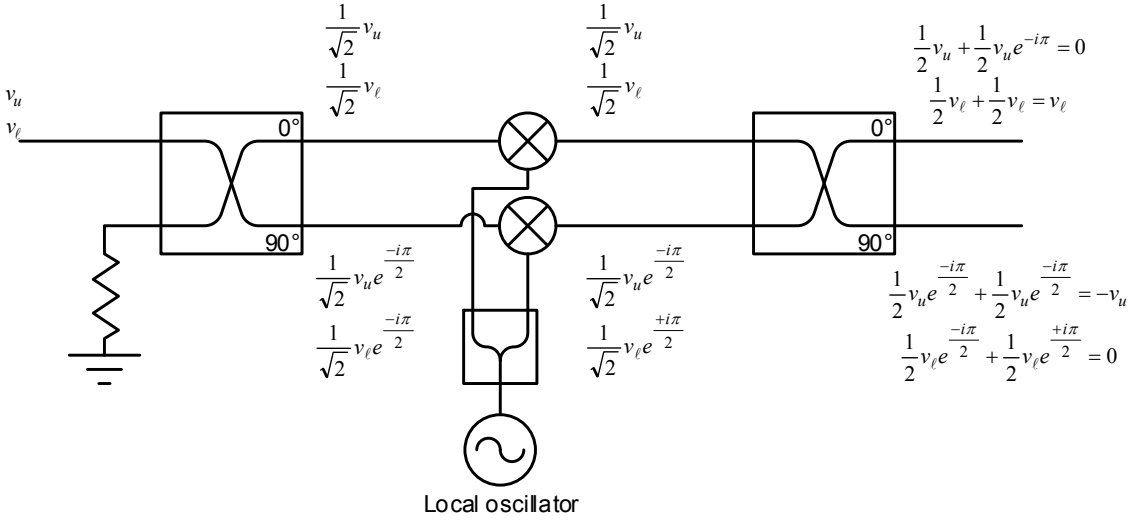

Figure 6. Principle of the sideband-separating mixer. The equations track the amplitude and phase of the upper and lower sideband voltages through the system, showing how the separation works under ideal conditions. Common scale factors (e.g., mixer conversion loss) and frequencies are suppressed for clarity.

Figure 6 illustrates the operation of the sideband-separating mixer. It relies on the fact that the rotating phase of a signal going into a mixer causes the output signal to change by the same amount for the USB, and by the negative of that for the LSB. Since the waveguide hybrid produces a 90° phase shift, the USB and LSB have phase changes after the mixer of +90° and −90°, respectively. The output quadrature hybrid adds phase to give the sums and differences at the outputs, corresponding to the USB and LSB signals. For perfect operation, the quadrature hybrids should split the amplitudes equally, and the outputs should be in exact quadrature. Furthermore, the LO should be fed precisely in phase, and the mixer conversion losses should be perfectly matched. Any imperfections in components can be combined into a phase tracking error and an amplitude imbalance. The effects of these on the sideband rejection (separation) are shown in Figure 7.

We note that an alternative configuration is to split the signal in phase and introduce the required 90° phase shift in the LO. This has the advantage that the bandwidth of the quadrature hybrid is reduced by the maximum IF frequency, and that the mixer may be less sensitive to LO amplitude balance if it is close to saturation. The drawback is that the isolation in a lossless in-phase splitter is rather poor, which may compromise performance.

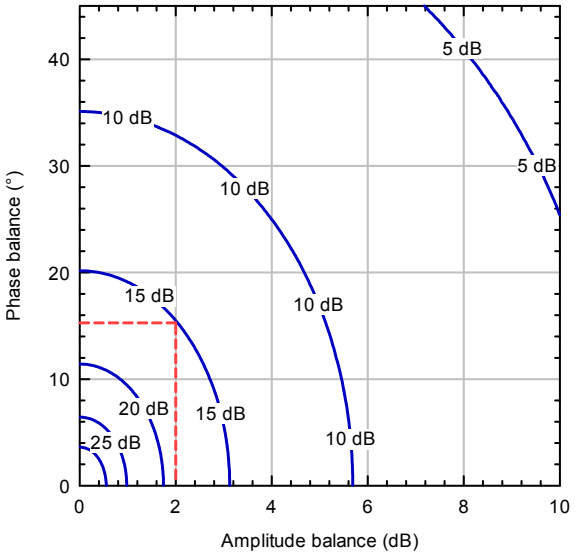

Figure 7. Map showing contours of constant image rejection for pairs of amplitude and phase imbalance. The red dashed lines indicate the goal for the CARMA receivers.

In an interferometer, the sidebands may be separated in the correlator. This applies only to the correlated astronomical signal, and not to any incoherent noise. The purpose of the sideband mixer is therefore primarily to reject the noise from the opposite sideband to improve system sensitivity. A sideband ratio (SBR) of 10 is sufficient to reduce the image noise by 90%. It should be noted that amplifier gain variations mean that the noise is not flat. A goal was adopted to have a rejection ratio of 15 dB, so that even if the image noise were 5 dB higher than in the signal band, it would still be reduced to 10% of the signal sideband noise.

The design goal of 15-dB rejection was divided into an amplitude imbalance of ~ 2.5 dB and a phase imbalance of ~ 15°. Table 1 lists the main components with their share of the amplitude and phase budget.

Table 1. Amplitude and phase tracking error budget goals for the sideband-separating mixer.

Component	Amplitude, dB	Phase, °
Waveguide quadrature hybrid	±1.5	1.5
Mixers	±2.0	5.0
LO splitter	±0.1	1.5
IF cables	±0.1	10.0
IF hybrid	±0.5	10.0
Total (RSS)	±2.5	±15.1

Since this budget is tight, it was decided to include a phase (delay) adjuster in one of the IF cables, and a fixed pad in the other to allow for some tweaking of the balance during assembly.

3.1 Waveguide quadrature hybrid

Wideband quadrature hybrids have been described by Srikanth and Kerr[7], and Andoh et al.[8, 9], both using a branchline configuration, with six and five branches, respectively. This geometry is illustrated in Figure 8. While the phase performance of this type of hybrid is intrinsically close to ideal, the performance improves with the number of branches. However, the amplitude balance does not approach the ideal flat 3 dB split regardless of the number of branches. In addition, the branch heights get smaller and harder to fabricate. With the machining tolerances available, we concluded that the optimum number of branches was eight.

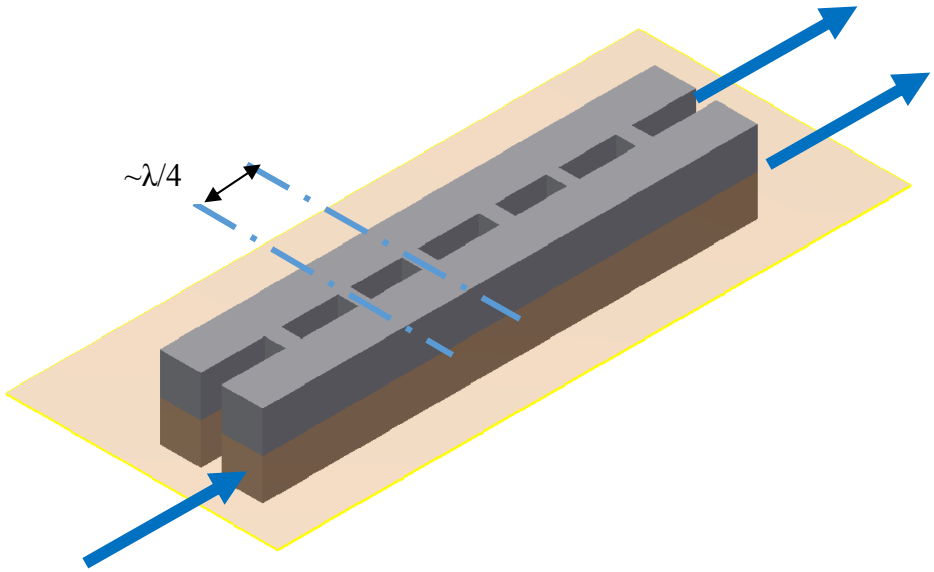

Figure 8. Design of a branchline coupler. The branches between the input waveguide and the coupled guide are spaced roughly a quarter-wavelength apart. The number and height (narrow dimension) of the branches controls the amplitude coupling to the other guide.

Previous designs of quadrature hybrid used a split block approach, so that the aspect ratio of the slots in each half is half the waveguide width to the branchline height. To get round this limitation, we used the construction shown in Figure 9, where the branches are machined into a septum plate between the two waveguides, and the aspect ratio is the branchline waveguide height to length which is appreciably smaller (ideally < 5). (Note that the branchline 'height' is the dimension parallel to the E-field.) This requires that the waveguide corners are rounded, rather than square, but simulations showed that this did not have any significant effect.

A full optimization was done using QuickWave (QWED Sp. z o.o.), allowing both the spacing and heights of the branches to vary. This contrasts with the references mentioned above, where only the spacing[7], *or* height[9] were adjustable. A comparison between the predicted performance of the designs in the references, and the design presented here is plotted in Figure 11.

One of the fabrication techniques tested was laser-machining of the slots in the septum. Machining from one side resulted in a tapered groove, compromising the performance. A second run, machining from both sides to improve symmetry also did not produce a satisfactory result. The final method was machining with a 65 000 rpm air spindle, which produced acceptable dimensions and surface finish. Naval brass sheet was used for the septum, and the final electromagnetic design optimization used the actual measured thickness of the material.

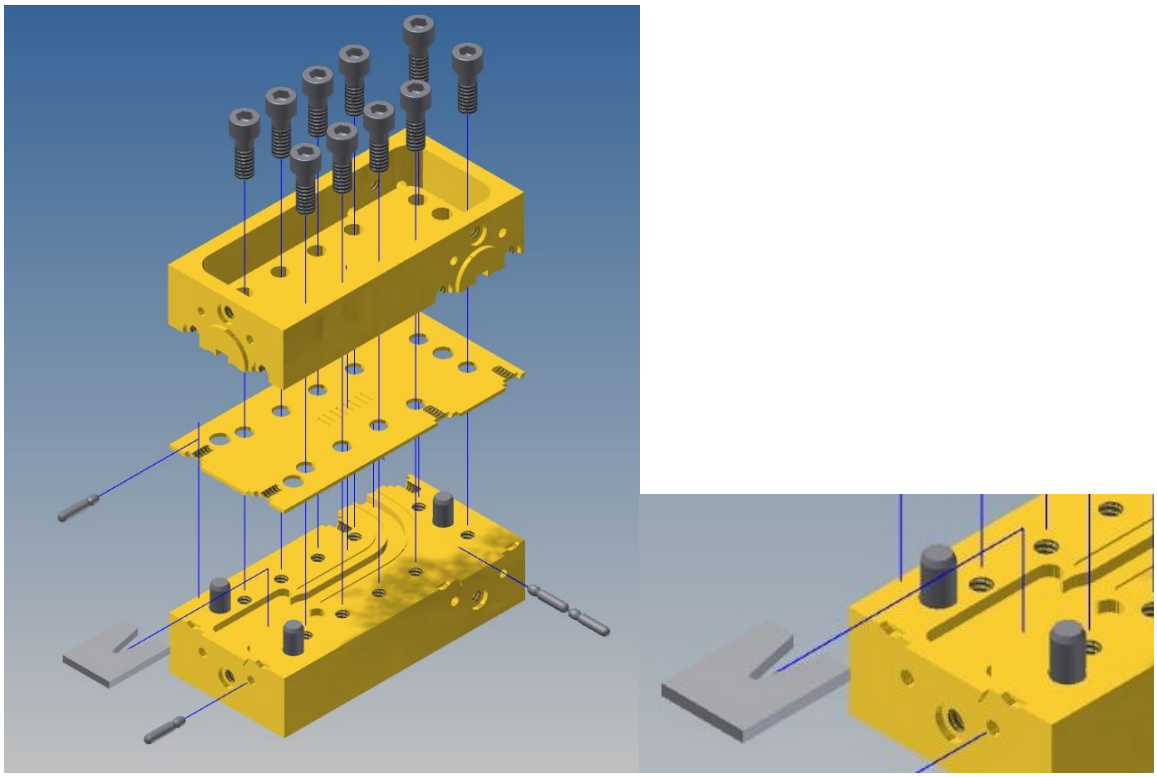

(a) (b)

Figure 9. (a) Construction of the CARMA waveguide hybrid coupler, and (b) detail of the waveguide termination.

Measurements of the slots were made with a microscope and digital camera, and the images analyzed with a LabVIEW (National Instruments) program. Results given in Figure 10 show the improvement in process control and that the tolerances of < 5 μm were achievable.

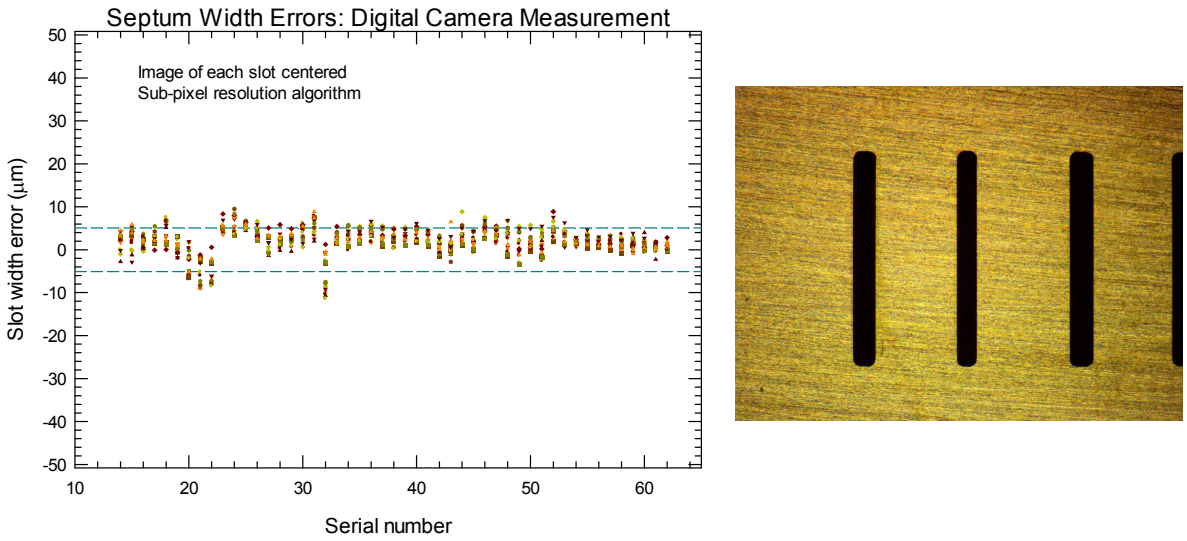

Figure 10. Measurements of the eight slots (top and bottom) for the series of slotted plates that form the branchlines in the coupler. The photo on the right shows typical machined slots.

A novel waveguide load was designed for the unused port termination. It consists of a slab of Eccosorb MF 110 (Emerson & Cuming) absorber with a V-slot, mounted at the end of the waveguide. The waveguide is widened before the absorber, making the absorber relatively large and rugged, and easy to machine compared to more conventional tapered cones or triangles in standard waveguide (Figure 9).

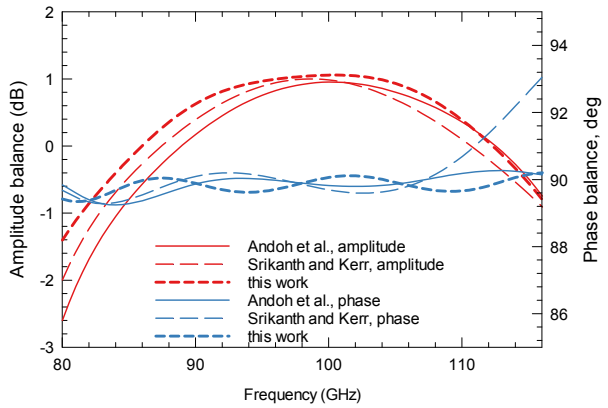

Figure 11. Comparison of the predicted performance for the designs referenced in the text, and this work.

Measurements of one of the quadrature hybrids are shown in Figure 12, demonstrating that the performance is very close to the simulations in HFSS.

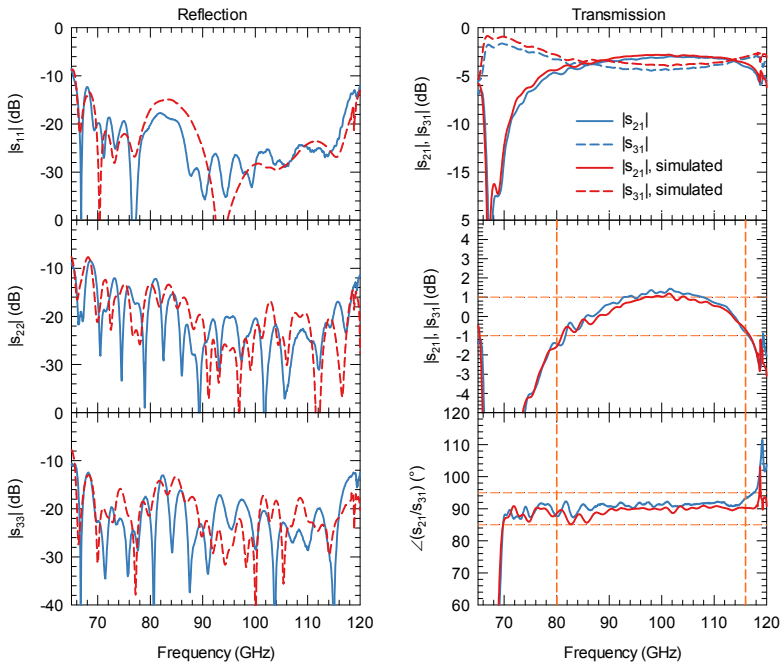

Figure 12. Measurements of a typical quadrature hybrid. The *s*-parameters from the simulation are compared with those measured on a VNA.

3.2 Waveguide LO splitter

Tight integration and stringent amplitude and phase match requirements mandated a custom waveguide splitter. This allowed the geometry to be adapted to the required positioning of the mixers. A split block construction was adopted as shown in Figure 13. The first split is to the two polarizations, and then each polarization has a split for the two mixers. This second split has strict phase match requirements to meet. Firstly, the geometry was carefully laid out so that the two paths were essentially identical in terms of all the bend radii and straight section lengths. Just having identical total guide lengths was found to be insufficient, since slight differences in the locations of the bends gave small reflections with different phases. Secondly, the depth of the cut (the waveguide width direction) had to be matched to better than 5 μm, otherwise differences in guide wavelength gave rise to excessive phase errors. Special tooling was developed to guarantee the flatness of the block during machining.

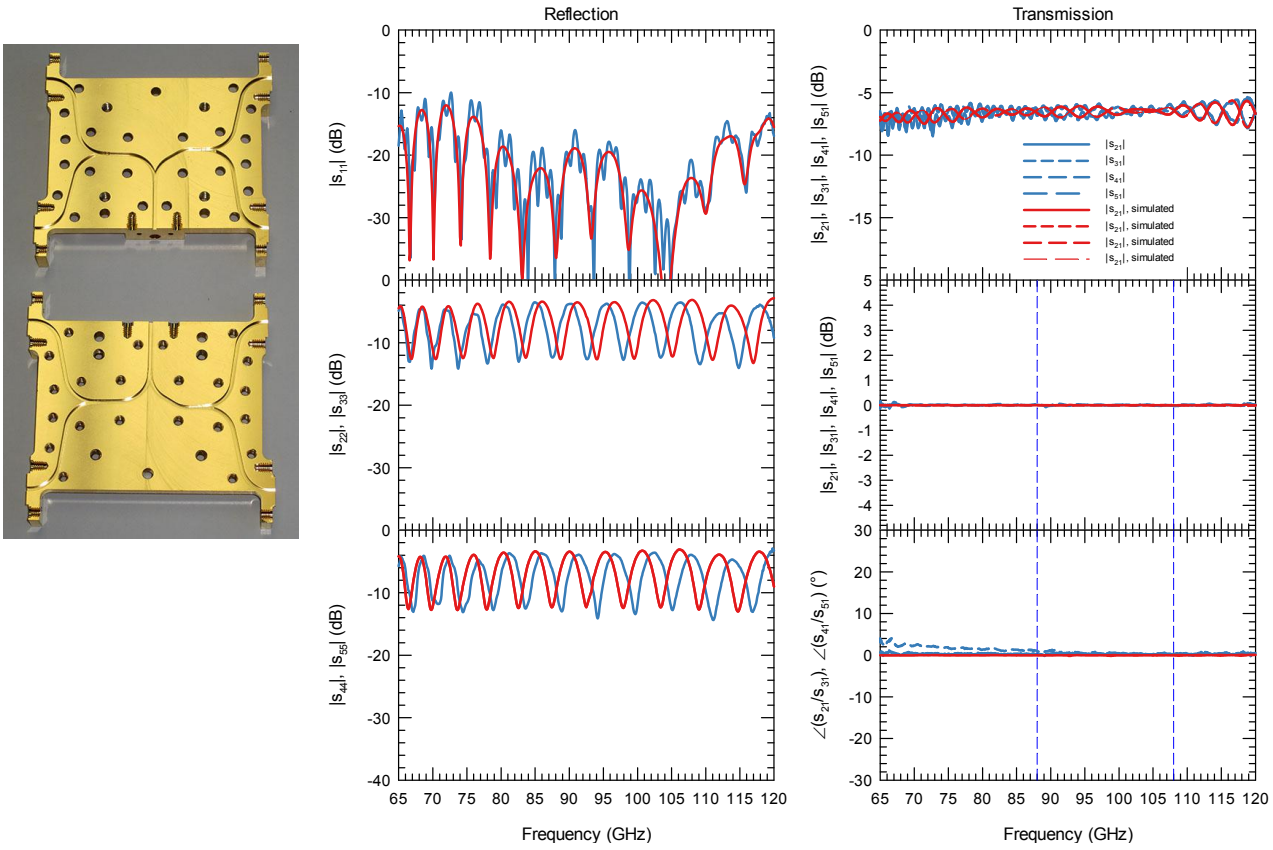

Figure 13. The photo on the left shows the split-block construction of the waveguide LO splitter. On the right are measurements of the *s*-parameters (blue) along with the simulated results (red).

3.3 Mixers

Commercial mixers from Millitech were found to meet the phase and amplitude requirements. These were model MB-10 biasable balanced mixers, which have lower LO drive requirements than the unbiased version, allowing the existing CARMA LOs to be used without additional amplifiers.

A test set was developed to make relative phase and amplitude measurements for pairs of mixers, yielding a dataset that could be used to find the optimum mixer pairing. The resulting data are graphed in Figure 14

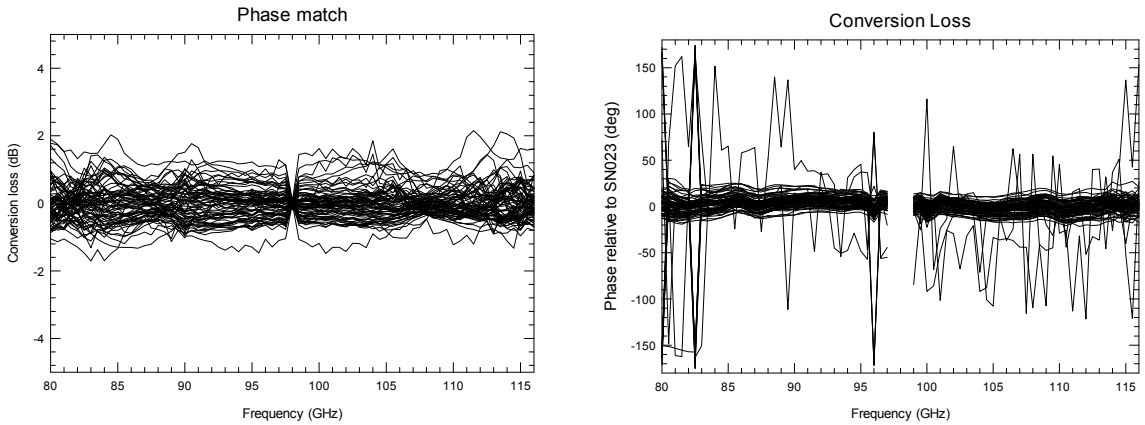

Figure 14. Phase and amplitude match measurements for over 70 mixers are shown.

Some investigation of the mixer conversion loss and phase on bias showed that there was some potential for optimizing for a particular frequency, but the dependence is complicated enough not to be a particularly attractive option.

3.4 IF hybrids

Krytar model 1831 1–18 GHz hybrids with the enhanced phase match option were used for the IF hybrid. A typical VNA (vector network analyzer) measurement is given in Figure 15, with the specification phase balance indicated on the plots. It is important to note that the standard specification for quadrature hybrid amplitude match is each port relative to the mean, rather than between ports. The phase tracking error typically has a linear (delay) term that can be compensated so that the phase match can be improved over the nominal specification.

3.5 Phase adjusters

Phase adjusters from Spectrum Electrotechnik GmbH (model LS-0085-02) were used in one IF port between the mixer and hybrid. The other arm had a fixed length of cable with a delay equal to the mid position of the adjustable one.

3.6 Pads

Both IF lines have a location for an attenuator to equalize the gains. Typically, one arm would have a pad of 0, 1, or 2 dB, and the other a 0-dB pad to maintain phase match. This allows the average gains to be matched to better than ±0.5 dB.

3.7 Dual-polarization sideband separating assembly

An illustration of the full dual-polarization sideband separating assembly is given in Figure 16. The mixers are attached to the quadrature hybrids on opposite sides of the branchline septum, so the LO flanges are correspondingly offset. This is matched by an corresponding offset in the LO splitter waveguide flanges for the mixers. This avoids extraneous waveguide sections with the associated tolerances in matching.

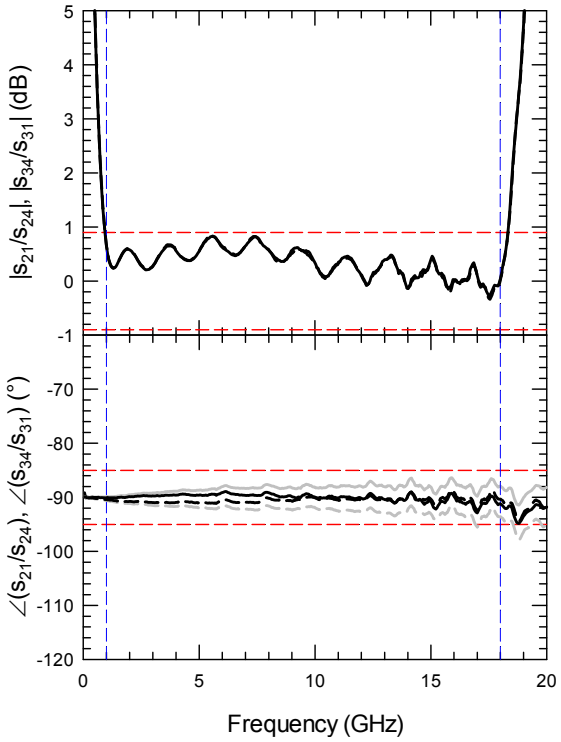

Figure 15. Amplitude and phase match measurements of a Krytar model 1831 stripline quadrature hybrid. The red lines denote the specification limits. In the phase plot, the grey lines are the measurements, and the black lines have a delay term removed, since that can be accomplished with a phase adjuster.

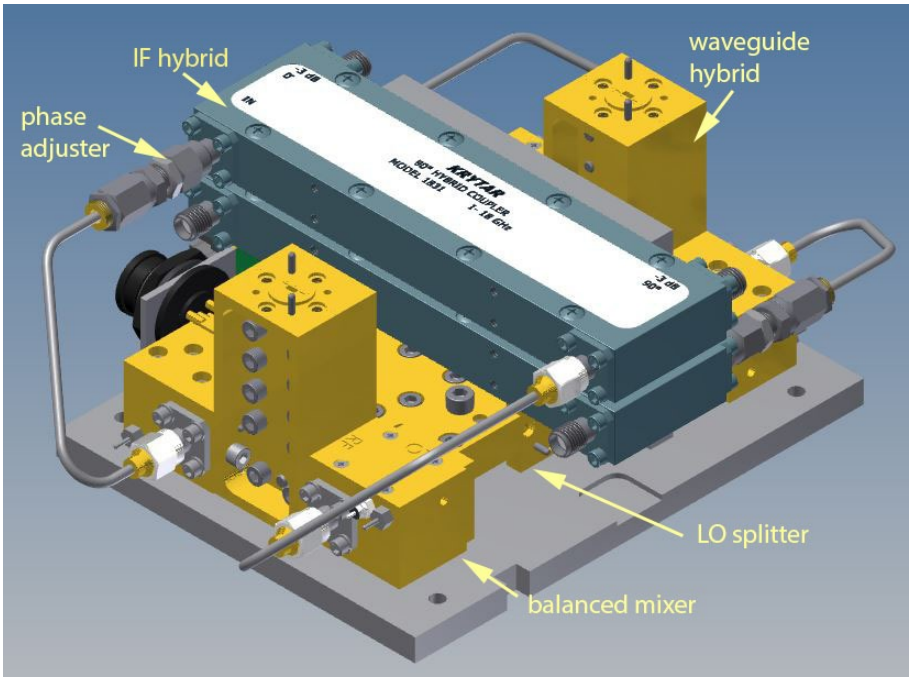

Figure 16. A solid model rendering of the final sideband-separating mixer assembly. The outputs from the two MMIC amplifiers enter through the waveguide ports on the tops of the quadrature hybrids, and the LO through a port in the LO splitter, just below the IF hybrids.

3.8 Performance

Using a synthesizer followed by a ×6 multiplier and attenuator to give ~0 dBm output, we characterized the prototype sideband-separating mixer. Two configurations were tested. In the first, the LO was fixed at 98 GHz, and a 1–18 GHz amplifier (Mini-Circuits ZVA-183S+) IF represented the final configuration. In the second, a 1–14 GHz amplifier (Mini-Circuits ZX60-14012L-S+), followed by the standard CARMA 1–9 GHz amplifier module, was used for the bachward-compatibe configuration.

With some small correction of the phase adjuster, good sideband rejection was obtained across the whole band (Figure 17).

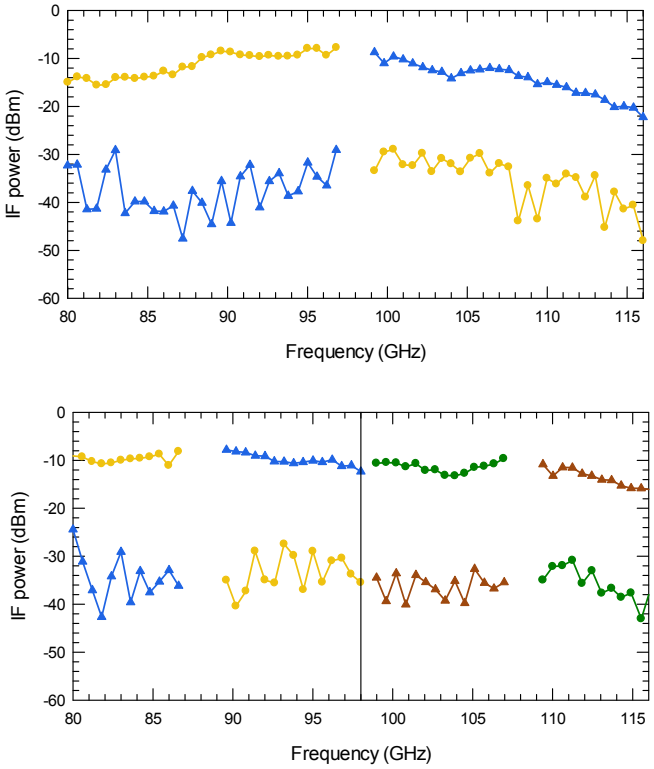

Figure 17. Measurements of the first sideband-separating mixer. In the upper plot, the LO is at 98 GHz, and the full 1–18 GHz IF is utilized. The lower plot shows two LO settings that cover most of the band with the legacy 1–9 GHz IF. In all cases the response of all the ports is shown for the signal and image sidebands. The difference between the two ports for a given sideband is a good measure of the rejection ratio, typically > 15 dB.

4. RECEIVER

A first version of the receiver was built in an OVRO 4-K dewar. This temperature is required for the 1-mm SIS receiver in the same dewar, but it does give a small, but measurable, improvement in noise temperature relative to the initial test system at 27 K (Figure 5). The full receiver was implemented, including the horn, polarizer, OMT, two amplifier modules, and a dual-polarization sideband-separating mixer.

In addition to the above components, we included waveguide isolators (Millimeter Wave Products model 115W/387) between the waveguide windows and the quadrature hybrids to control standing waves in the long output waveguide sections. All of the testing was done with the isolators in situ.

After testing in the lab, the receiver was deployed on one of the 10.4-m CARMA antennas to cross-correlate with the existing SIS receivers. With the circular polarizer installed, there was an equal correlation of the two circular polarizations with the other, single-linear polarization receivers, indicating both circular polarization channels were operating as expected. After a short period in this configuration, the circular polarizer was replaced with a straight section of circular guide, and observations continued with a single linear polarization.

4.1 Noise temperature

Noise temperatures were measured using an ambient and a liquid nitrogen (LN) cold load. The cold load was downward looking in a polystyrene container, and its effective radiation was taken to be 80 K (from a comparison with a LN saturated conical load). Presented in Figure 18, the measurements show an SSB noise temperature between about 40 K and 70 K. In this, it was assumed that sideband separation was perfect, but this is a rather small correction.

On the sky, the system noise temperatures could be compared directly with the existing receivers under various observing conditions. Under poorer conditions, the advantage of the single-sideband receiver is greater. From the measurements, we deduced that the improvement in sensitivity for two MMIC receivers vs. two SIS receivers would typically be about 60% for spectral line observations.

The existing IF co-axial switches were configured so that the USB or LSB could easily be selected remotely.

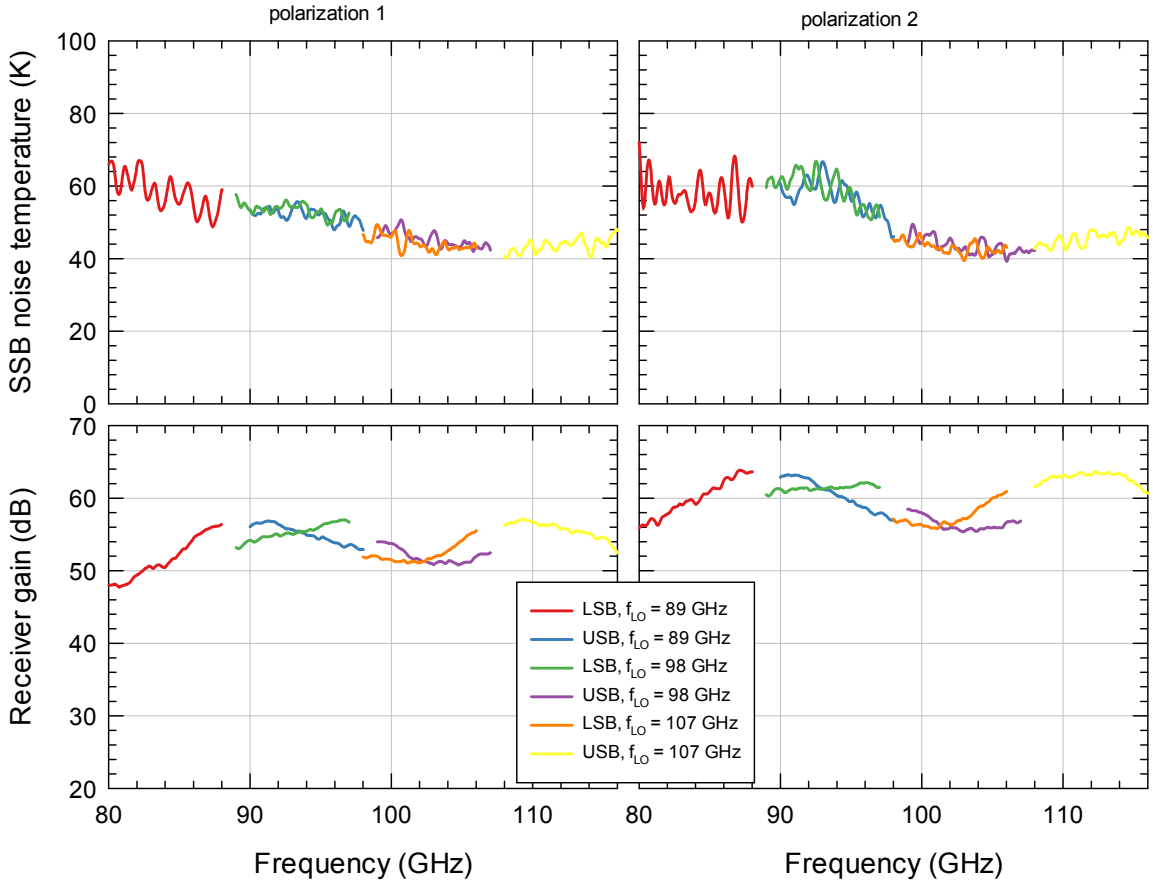

Figure 18. Noise temperature and gain for the two polarizations made in the lab using a LN cold load before installation on the telescope. Several LO tunings are shown, with the IF in the 1–9 GHz band.

4.2 Sideband ratio

Using the correlator on the array, the sideband ratio was determined on astronomical sources. Measurement on continuum sources, such as 3C84, gave an estimate of the sideband ratio across the receiver passband. These are shown in Figure 19. The cause of the ripple in the rejection ratio is still not understood. As a double check, a measurement was made of a maser in Orion, which is very bright in one sideband, and this was in agreement with the continuum measurements. Lab measurements were made to try to shed some light on this.

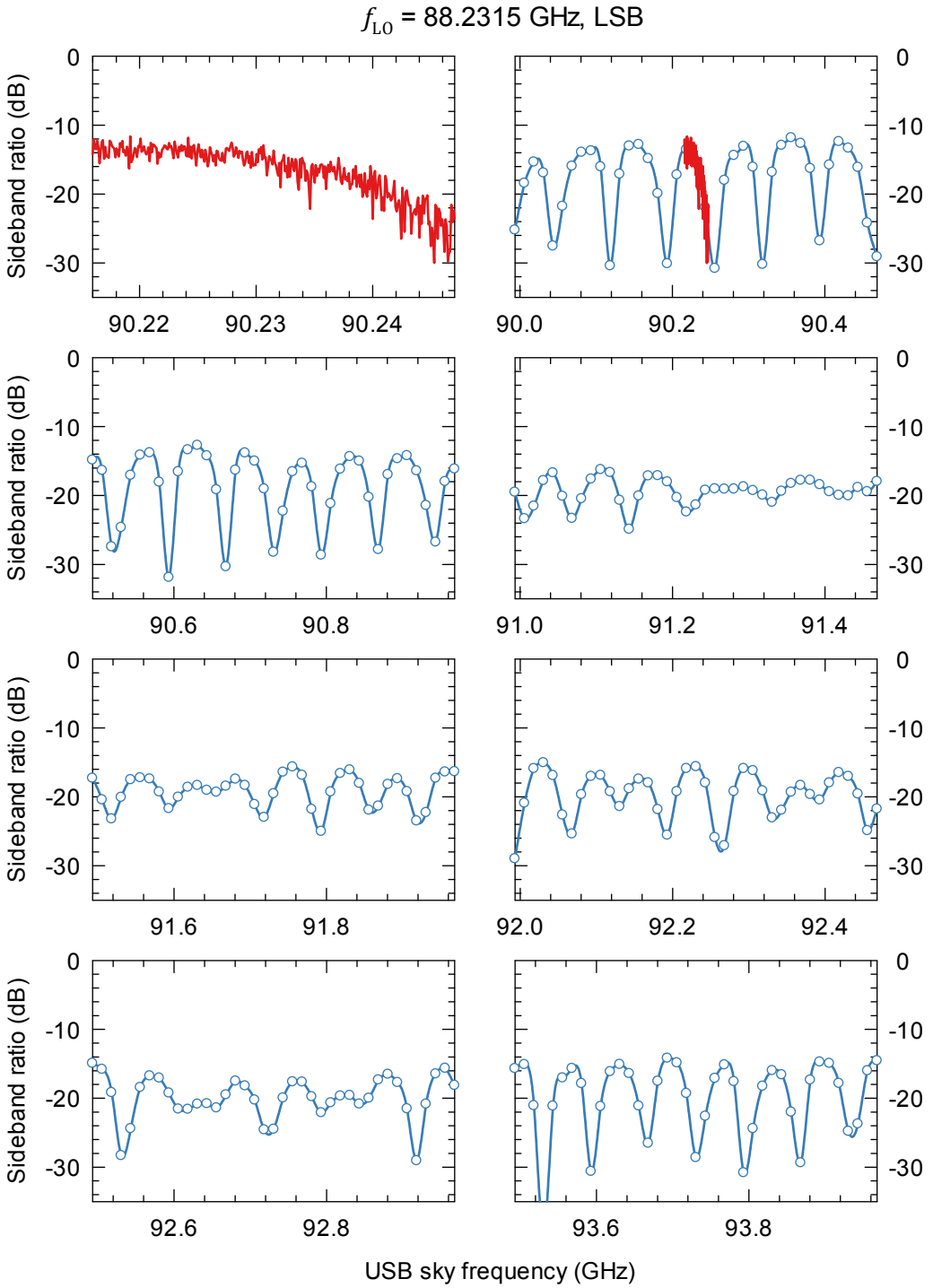

Figure 19. Measurements made with the eight CARMA spectral-line correlator bands spread out over the 1–9 GHz IF. The symbols correspond to the spectral channels within each band. The upper-left panel corresponds to a high resolution configuration that overlaps the wideband configuration in the upper-right panel. The high resolution band is superimposed on the wideband data in the latter plot.

When removed from the telescope, the receiver was tested in the lab with the multiplied synthesizer source injected through the dewar window. The signal was attenuated so that the receiver would operate in the linear range, and free-space absorber was used to reduce reflections from surroundings. The rejection was calculated as the ratio of the signal in the nominal sideband channel to the signal in the image sideband channel. This assumes that the IF amplifiers have the same gain, which introduces a negligible error.

It may be seen that there is a lot of structure in the data. While this remains unexplained, it does confirm that the sideband ratio is typically better than 15 dB

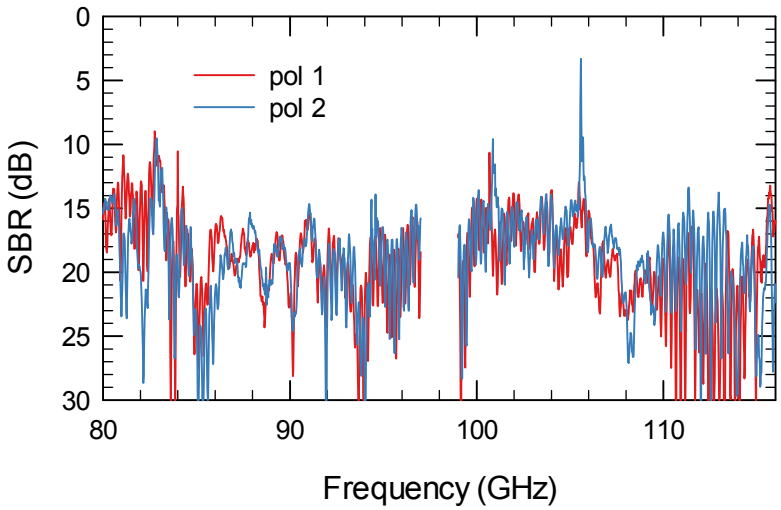

Figure 20. Results of lab measurements of the sideband ratio (SBR) of the receiver in both polarizations.

5. DISCUSSION AND CONCLUSIONS

A full prototype receiver using cryogenic MMIC amplifiers and sideband separating mixers was designed, constructed and tested for use in CARMA. The performance on the telescope showed a significant gain in sensitivity compared to the existing SIS mixer receivers. Typically, the receiver noise temperature was between 40 and 70 K, and in particular, at the critical line frequency of CO at 115.3 GHz, less than 50 K. The goal for sideband rejection was 15 dB, and this is clearly met in the sideband-separating mixer. However, there is apparently some interaction with the receiver that introduces some structure into the rejection vs frequency. The cause of this is as yet unknown, but the receiver on the telescope consistently exhibits image rejection better than 12 dB.

While many components were fabricated or purchased, no more receivers have been built because of the termination of funding for CARMA. We expect to be able to continue with other projects however, and the goal is to be able to utilize the entire bandwidth, using better optical links and new correlators. An exciting prospect is to improve the sideband rejection by dispensing with the IF hybrid and combining the signals in the correlator with appropriate complex weights. There may be some advantage in retaining the hybrids, and simply using the correlator to refine the rejection.

ACKNOWLEDGEMENTS

We would like to acknowledge the invaluable work done by Mr. Stan Hudson at the Owens Valley Observatory machine shop in machining many of the parts described here. In particular, it took great perseverance to refine the process for machining the slots for the quadrature hybrids.

Support for CARMA construction was derived from the Gordon and Betty Moore Foundation, the Kenneth T. and Eileen L. Norris Foundation, the James S. McDonnell Foundation, the Associates of the California Institute of Technology, the University of Chicago, the states of California, Illinois, and Maryland, and the National Science Foundation. CARMA development and operations were supported by the National Science Foundation under a cooperative agreement (grant AST-1140063), and by the CARMA partner universities.

REFERENCES

[1] Woody, D. P., Beasley, A. J., Bolatto, A. D., Carlstrom, J. E., Harris, A., Hawkins, D. W., *et al.*, "CARMA: a new heterogeneous millimeter-wave interferometer," Proc. SPIE, (2004).

[2] Varonen, M., Larkoski, P., Fung, A., Samoska, L., Kangaslahti, P., Gaier, T., *et al.*, "160-270-GHz InP HEMT MMIC Low-Noise Amplifiers," 2012 IEEE Compound Semiconductor Integrated Circuit Symposium, (2012).

[3] Reeves, R., Cleary, K., Gawande, R., Kooi, J., Lamb, J., Readhead, A., *et al.*, "Cryogenic Probing of mm-Wave MMIC LNAs for Large Focal-Plane Arrays in Radio-Astronomy," 2014 9th European Microwave Integrated Circuit Conference (Eumic), 580-583(2014).

[4] Lamb, J. W., "Evaluation of biasing and protection circuitry components for cryogenic MMIC low-noise amplifiers," Cryogenics, 61(0), 43-54(2014).

[5] Plambeck, R. and Engargiola, G., "Circular polarizers for the CARMA 1mm receivers," CARMA Memorandum Series 54 (2010).

[6] Henke, D. and Claude, S., "Design of a 70-116 GHz W-band turnstile OMT," Microwave Conference (EuMC), 2014 44th European, 456-459, (2014).

[7] Srikanth, S. and Kerr, A. R., "Waveguide quadrature hybrids for ALMA receivers," ALMA Memo 343 (2001).

[8] Andoh, H., Asayama, S., Ogawa, H., Mizuno, N., Mizuno, A., Tsukamoto, T., *et al.*, "Numerical matrix analysis for performances of wideband 100GHz branch-line couplers," International Journal of Infrared and Millimeter Waves, 24(5), 773-788(2003).

[9] Andoh, H., Minamidani, T., Asayama, S. i., Yonekura, Y., Ogawa, H., Mizuno, N., *et al.*, "Designs of wideband 3dB branch-line couplers for ALMA bands 3 to 10," 468 (2003).